IRREVERSIBILITY AND MOLECULAR DYNAMICS*. II.

William G. Hoover

Department of Applied Science; University of California at Davis
and
Department of Physics; Lawrence Livermore National Laboratory
Livermore, California 94550 USA

*. This work was performed under the auspices of the United States Department of Energy under University of California-Lawrence Livermore National Laboratory Contract Number W-7405-Eng-48.

Abstract:

In this second of a pair of papers I emphasize the impact of recent developments on the problem of understanding irreversibility, as summarized in the Second Law of Thermodynamics, and speculate on the applicability of these same ideas to quantum systems.

I. Irreversibility from Time-Reversible Many-Body Mechanics-Nosé's Modification of Hamiltonian Mechanics

Molecular dynamics replaced a generation of cumbersome, inadequate, approximate one-body and two-body theories with simple, accurate many-body computer experiments. But appropriate analyses of these experiments required new ideas suited to computation. This had to wait for a new generation of scientists brought up to use the computer as a tool, for which new techniques could be specially designed.

An advance was made by setting aside the irreversible stochastic approximations well-suited to slower hand calculations, but not so well-suited to understanding deterministic trajectory development far from equilibrium. The classical Langevin and Fokker-Planck equations had previously been used to impose temperature, but these approaches are time-irreversible. The simplest derivation of the Fokker-Planck equation[1], for instance, assumes an acceleration proportional to the momentum gradient of a local entropy:

$$\Delta(dp/dt) \propto \nabla_p\{\ln[f(p)/\mathbf{f_{equilibrium}}(p)]\}.$$

Reversing the sign of the time leaves the left side unchanged while changing the sign of the right side, revealing the time-*irreversible* approximate character of the Fokker-Planck equation.

Nosé, from Japan, but working in Canada with Mike Klein, made the necessary conceptual breakthrough. Nosé[2] discovered a reversible deterministic form of Hamiltonian mechanics which reproduces the thermal canonical distribution. His temperature-dependent reversible equations describe something like a microwave oven, but capable of cooling reversibly as well as heating. The Hamiltonian basis of his work is important for two different reasons. First, the equations of motion, either at or away from equilibrium, are time-reversible, making possible an exact analysis of thermodynamically-irreversible processes. Second, the Hamiltonian basis suggests extensions of Nosé's classical ideas to quantum dynamics and quantum statistical mechanics. Despite these two advantages, his original derivation was unnecessarily complex. But the result is simple, a set of many-body equations of motion, containing the equilibrium temperature T and at least one friction coefficient ζ:

$$dp/dt = F(q) - \zeta p \ ,$$

where the friction coefficient ζ, rather than being constant, is itself determined by a temperature-dependent time-reversible integral feedback equation:

$$d\zeta/dt = \sum [(p^2/mkT) - 1]/\tau^2 \ ,$$

with an arbitrary relaxation time τ. Thus the friction coefficient ζ increases in those parts of phase space with above-average temperature and decreases in those parts where the temperature is below average.

Nosé's derivation of his equilibrium equations of motion was relatively complicated. A simpler way to derive these same equations of motion is to ask the question Brad Holian posed: "What friction coefficient ζ generates the canonical distribution[3]?" A whole series of "Nosé-Hoover" equations of motion, based on the various velocity moments $\langle p^{2n} \rangle$ can similarly be derived[4].

At equilibrium, or in the nonequilibrium linear-response regime, Nosé's ideas simply reproduce Newtonian mechanics, with time-averaged macroscopic deviations of order 1/N for N-particle systems[5]. But Nosé's ideas can also be used to drive many-body systems away from equilibrium, with external forces, into thermostatted nonequilibrium steady states maintained by one or more Nosé thermostats[6]. Then concepts and methods borrowed from nonlinear dynamics can be used to determine and describe the structure of the resulting phase-space distributions. Once Nosé announced his discovery, Ashurst's work was recognized as a special case of Nosé's more-flexible feedback recipe.

At equilibrium Nosé discovered a new way to generate the equilibrium phase-space distribution f_N. In the more complex cases away from equilibrium, something more interesting happens. In any such case heat is exchanged. It can then be proved that *any* such nonequilibrium steady state *always* produces a *fractal* phase-space dimensionality, with an occupied phase-space dimension reduced below the equilibrium dimensionality[7-9]. The amazing result that these distributions *never* become continuous, no matter how fine the scale of observation, is, for the many-body problem, as exciting and surprising a development as was the discovery of chaos in mechanics. And *that* discovery, which dates back to Poincaré, is viewed by many as revolutionary for physics today[10-13].

What are these ubiquitous fractal objects that characterize nonequilibrium systems? Fractal objects have been used in films to represent mountains, clouds, and water. A recent computer-generated magazine cover using fractals as a tool, is shown in **Figure 1**. A simpler fractal object is the Sierpinski sponge[14], shown in **Figure 2**. In any fractal the number of pairs of points varies in a regular way with distance. If one defines a dimensionality for such an object, by asking for the number of pairs of points lying within a radius r, that dimensionality is typically *not* an integer. For the sponge of Figure 2 the number of pairs of points within a small distance r of each other varies as $r^{2.727}$. Thus the sponge is said to have fractal dimensionality of 2.727. The object behaves like a fractional-dimensional "fractal" object. That these strange objects describe phase-space flows was probably unknown to Boltzmann. They are beautifully illustrated and described in Gleick's book on Chaos[10].

Figure 1. Computer-generated snake or computer-generated fractal background

Figure 2. Sierpinski sponge generated from a cube by repeatedly removing 7/27 of the remaining mass. The mass remaining after N such removals is $(20/27)^N$. As N diverges the resulting object becomes a zero-volume fractal object with a fractal dimensionality of 2.727.

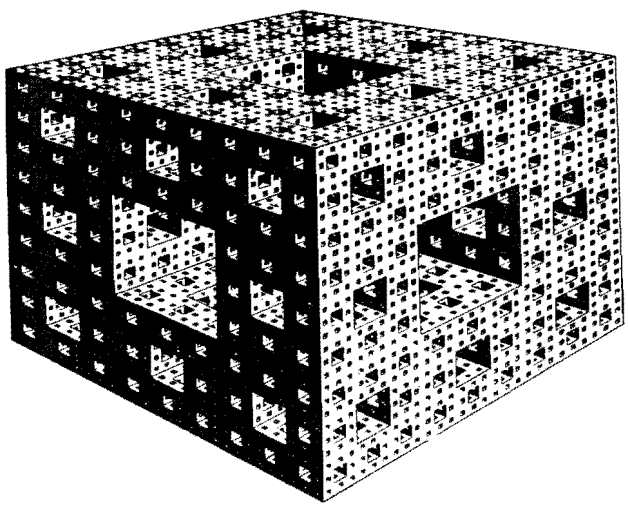

Developing and demonstrating these ideas required high-speed computer graphics. Even so, phase-space fractals are hard to display in the many-body case. About the simplest steady-state phase-space fractal distribution illustrates the one-body Galton-Board example[15] shown in **Figure 3**. In this example a single mass point falls through a periodic array of scatters. The accelerating "gravitational" field is downward, and the motion is made isokinetic, with the particle falling at constant speed, by applying Gauss' Principle of Least Constraint [4,15]. The resulting phase space is only three-dimensional. In the Figure a phase-space cross section representing 10,000 successive collisions is shown. The distribution of distances between pairs of points in the cross section is consistent with a fractal dimensionality of about 1.5.

Figure 4 shows two separate ensembles, each with 2500 separate Galton Boards developing in time. Initially the ensemble members are distributed uniformly over two quadrants of the square phase-space cross section. The successive images show the ensemble members after 1, 2, 3, 5, and 10 collisions. Note that the ensembles' cross sections are approaching the single-trajectory Poincaré section shown in Figure 3. Similar calculations have been carried out for a low-density shear-flow analog of the Galton Board, using both molecular dynamics[16] and the Boltzmann Equation[17].

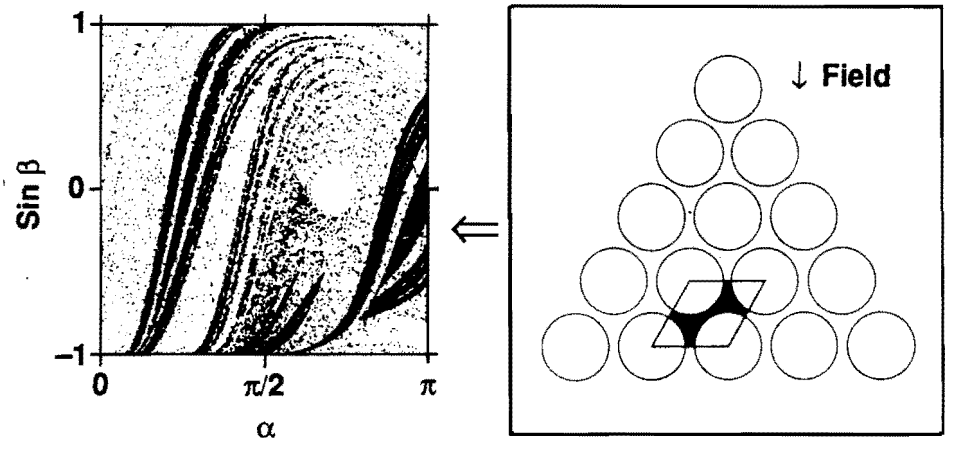

Figure 3. Galton Board trajectory Poincaré section showing the history of successive collisions for a single mass point moving through the board. The Board geometry and a unit cell are shown to the right. Each point in the phase-space section on the left indicates a collision. The abscissa angle α measures the location of the collision relative to the field direction. 0 and π correspond respectively to collisions at the bottom and the top of a scatterer. The ordinate measures the (sine of the) angle β, relative to the normal, of the moving particle's velocity after each collision. Glancing collisions correspond to angles of $\pi/2$ or $-\pi/2$. A head-on collision corresponds to $\beta = 0$. The "hole" corresponds to an exceptional and interesting isolated set of quasiperiodic Kolmogoroff-Arnold-Moser collisions which are not connected to the main chaotic phase space.

Figure 4. Two Galton Board ensemble Poincaré sections showing the time-development of two ensembles, each with 2500 mass points moving independently through Galton Boards of the same type, and with the same field as shown in Figure 3. The development of the ensembles after 1, 2, 3, 5, and 10 collisions is shown.

Nosé's idea, generalized to nonequilibrium systems, made possible the marvelous marriage of three parties, mechanics, nonlinear dynamics, and irreversible thermodynamics[7-9]. The new mechanics, with Nosé's computational thermostats built in, showed that nonequilibrium phase-space distributions are *typically* fractal, just like the one-body Galton Board problem illustrated above. The necessary geometric concepts are not so new. The basic idea of phase-space mixing was known to Poincaré and the mathematics of strange sets had been around for about fifty years when Nosé pointed the way toward a new synthesis.

With Nosé's dynamics the phase-space deformation of nonlinear dynamics, the heat reservoirs of nonequilibrium molecular dynamics, and the inexorable entropy increase of irreversible thermodynamics could all be linked together. The logical connections among these three concepts involve the three steps indicated in **Figure 5**:

(I). Conservation of comoving probability in mechanical phase-space flows, relating the time-rate-of-change of the many-body distribution function to the corresponding time-rate-of change of phase volume.

(II). Steady time-development of phase-volume from nonlinear dynamics, relating the sum of the Lyapunov exponents to the sum of Nosé's friction coefficients through Nosé's equations of motion.

(III). Linking the diminishing phase-space volume with thermodynamics through the heat reservoirs implicit in Nosé's equations of motion. This last step establishes that the impossibility of phase-space growth, in the steady state, is equivalent to the macroscopic Second Law of Thermodynamics.

Figure 5. Three steps linking mechanics, dynamics, and irreversible thermodynamics.

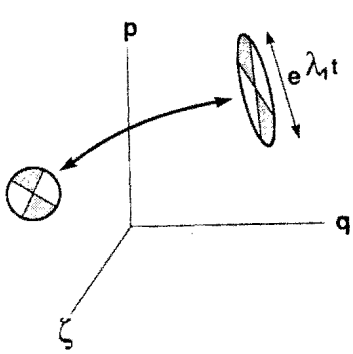

I and II:
$d\ln f/dt + d\ln\otimes/dt \equiv 0;$
$\Sigma\zeta + \Sigma\lambda \equiv 0;$

III:

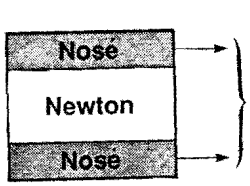

$\Sigma\lambda < 0 \Rightarrow \Sigma\zeta > 0.$

$\Sigma\left[\frac{dQ/dt}{T}\right] = \Sigma\zeta = \frac{d(S/k)}{dt}$

To begin with step **I**, *any* mechanical flow in phase space satisfies a "continuity equation", with conservation of the total number of systems studied. To illustrate, consider the continuity equation of fluid mechanics,

$$\partial\rho/\partial t + \partial(\rho u)/\partial x = 0 ,$$

where ρ is the mass density and u is the stream velocity. The typical textbook derivation of the continuity equation proceeds by setting the change in mass in a fixed "Eulerian" volume element dxdydz equal to the flow through the boundaries. This flow is proportional to the flux ρu. The only additional assumptions required to derive the continuity equation are (i) the differentiability of the flow velocity and density and (ii) the lack of sources or sinks. From the continuity equation the *comoving* density derivative (that is, the "Lagrangian" derivative following the motion) can be computed:

$$d\rho/dt = \partial\rho/\partial t + u(\partial\rho/\partial x) = -\rho(\partial u/\partial x) ,$$

Dividing by the density gives a more elegant logarithmic form:

$$d\ln\rho/dt = -(\partial u/\partial x)$$

The divergence of the velocity, $\partial u/\partial x$, the sum of the orthogonal strain rates, is also the logarithmic rate volume change:

$$(\partial u/\partial x) = d\ln V/dt .$$

Thus the continuity equation for fluid flow takes the form:

$$d\ln\rho/dt = -d\ln V/dt .$$

or

$$d\ln\rho/dt + d\ln V/dt = 0.$$

Exactly the same idea can be applied to the flow of many-body probability fluid in the many-body phase space. In that case the density function ρ is replaced by the N-body probability density f_N and the volume V is replaced by the 6N-dimensional phase-space hypervolume ⊗. Then the corresponding "continuity" equation for the flow of phase-space probability can be written

$$d\ln f_N/dt + d\ln\otimes/dt = 0 , \qquad (I)$$

where $f_N\otimes$ is the total number of systems in the phase-space hypervolume ⊗.

In the second step II above, the Lyapunov exponents used in analyzing many-dimensional flows[18] are introduced in order to describe the time-averaged expansion and contraction of the phase-space volume $\otimes$. The exponents give the time-averaged rates of stretching and shrinking of the principle axes of a deforming hyperellipsoid in the phase space. In nonlinear chaotic systems the stretching and shrinking occur *exponentially* fast in time, varying as $\exp[\lambda t]$. See again the last Figure in Paper I of this pair of papers. The sum of these exponents $\{\lambda\}$ gives the rate at which phase-space volume changes:

$$d\ln\otimes/dt = \sum\lambda \, .$$

Nosé's equations of motion satisfy identically the relation

$$d\ln f_N/dt = \sum\zeta \, .$$

Combining these results with (I) above relates Nosé's friction coefficients to the Lyapunov exponents:

$$\sum\zeta = d\ln f_N/dt = -d\ln\otimes/dt = -\sum\lambda \, . \quad (II)$$

Nosé's equations of motion also show directly that the time-averaged friction coefficients $\langle\{\zeta\}\rangle$ and the corresponding instantaneous temperatures $\langle\{p^2/mk\}\rangle$ are uncorrelated:

$$\sum\langle\zeta p^2/mk\rangle = \sum\langle\zeta\rangle\langle p^2/mk\rangle$$

Thus, the lefthand side, the summed rates of heat extraction of the Nosé thermostats divided by the corresponding temperatures, $\{\langle p^2/mk\rangle\}$, is exactly equal to the sum of the Nosé friction coefficients. The last step III, then links dynamics to the Second Law of Thermodynamics through the friction coefficients $\{\zeta\}$ in Nosé's equations of motion:

$$-d\ln f_N/dt = -\sum\zeta = -(dS/dt)/k \quad , \quad (III)$$

where the sum is over all such friction coefficients. The observation that the steady logarithmic rate of volume change, $d\ln\otimes/dt$, cannot be positive, and must vanish at equilibrium, leads to the conclusion

$$0 > d\ln\otimes/dt$$

away from equilibrium. This continuous decrease of phase-space volume in the nonequilibrium steady state establishes that Gibbs' equilibrium N-body entropy definition, $S = -k\langle\ln f_N\rangle$, cannot be used in such nonequilibrium steady states because the corresponding nonequilibrium S would approach minus infinity.

The steadily-decreasing phase-space hypervolume implies the full chain of relations

$$(dS/dt)/k = \sum\zeta = +d\ln f_N/dt = -d\ln\otimes/dt = -\sum\lambda > 0.$$

The resulting conclusion

--THE TOTAL ENTROPY MUST INCREASE--

is made possible only through the simple structure of the Nosé equations of motion. This total entropy includes that of the heat reservoirs in which any Nosé system is embedded. The Gibbs' entropy *diverges* for any nonequilibrium steady state. To see this, notice particularly that the many-body probability density $f_N(q^N,p^N,\zeta,t)$ diverges[8]. The Second Law of Thermodynamics, from the standpoint of Nosé mechanics, becomes equivalent to the observation that a steady-state distribution function must occupy a Lyapunov-unstable *subspace* with reduced dimensionality, a zero-volume "strange attractor". For such nonequilibrium systems, the Second Law of Thermodynamics is not simply a high-probability statement, as with Gibbs' Paradox, but instead a probability-one statement. This follows from the fact that the nonequilibrium distributions are zero-volume fractal objects.

To see this consequence of the fractal many-body distributions in more detail, consider time reversibility and Loschmidt's Paradox. Because the many-body equations of motion are time-reversal-invariant it is certainly true that the phase space must also contain a reversed "repellor" region, just like the attractor but with reversed velocities, in which the Second Law is violated. Despite the undoubted existence of the repellor the Second Law *cannot* be violated by observable motions[7-9]. This is because the reversed "repellor" solution repels rather than attracts nearby trajectories, and thereby acts as a phase-space *source* rather than a *sink*. It is an *unstable* phase-space object. Hence the reversed repellor trajectories, which would theoretically violate the Second Law of Thermodynamics, can never be observed using Nosé's mechanics.

Thus Nosé's mechanics sheds new light on, and extends, Boltzmann's treatment of irreversible processes. In this extension, the relevant distributions are many-body rather than one-body distributions. The underlying dynamics is the exact many-body dynamics rather than Boltzmann's approximate one-body dynamics. With Nosé's mechanics the statements that (1) entropy production is positive, that (2) heat flows from hot to cold, and that (3) transport coefficients are positive, all correspond to rigorous consequences of the equivalent geometric observation that phase-space hypervolumes cannot grow in nonequilibrium steady states.

Of course, Nosé's treatment of nonequilibrium boundaries is not the only possible treatment. But it is important to recognize that hydrodynamic flows can be generated and maintained by a variety of equally-valid boundary conditions. Those features that are common to a variety of boundaries will be shared by Nosé's choice. His is simply the most useful because it simplifies the corresponding theoretical analysis.

II. Speculation: Quantum Irreversibility using "Gaussian" Time-Reversible Schrœdinger Mechanics.

Gauss formulated mechanics on the basis of a single principle, his "Principle of Least Constraint"[19]. Gauss' Principle states that *any* dynamical constraint should be implemented by using the least possible force:

$$\Sigma(F_c^2/2m) \text{ minimum, or } \Sigma(F_c \delta F_c/m) = 0 \ .$$

The sum runs over all degrees of freedom in the constrained system.

It is interesting that this Principle, when used to implement isothermal conditions, by constraining the kinetic energy, produces exactly the same motion equations

$$dp/dt = F - \zeta p \ ,$$

as does Nosé's isothermal mechanics, but with a definite value for Nosé's relaxation time τ, zero.

The current interest in chaos has led to extensive speculation on "quantum chaos", that is the quantum behavior of systems with classically-chaotic Hamiltonians[13,20]. The Schrœdinger equation is not well suited to these studies so that a variety of efforts have been made to extend it to apply to nonequilibrium open systems[21-23].

First, the Schrœdinger Equation is linear, so that steady solutions can only oscillate in time. Second, it describes only thermally-isolated systems, while the simplest interpretations of irreversibility in classical systems involve open systems in which work is converted to heat through the operation of Nosé thermostats.

We can take Gauss' least-constraint idea[19] over into quantum mechanics by restricting the solution of a *constrained Schrœdinger Equation*, which incorporates the least possible change in the quantum equation of motion

$$(\partial\psi/\partial t)_{Gauss} = (\partial\psi/\partial t)_{Schrœdinger} - \Sigma(\lambda_I \nabla C_I) \ ,$$

where the $\{\lambda_I\}$ are Lagrange multipliers chosen to satisfy the constraints $\{C_I\}$.

To illustrate, consider the quantum version of the simple problem introduced in Figure 3, a mass point moving through a Galton Board under the influence of an external field[15]. Then the Gaussian constraints $\{C_I\}$ correspond to fixing the total mass, momentum, and energy in the Board. The Gaussian Lagrange multipliers $\{\lambda_I\}$ perform work and extract heat. The steady-state nonequilibrium Schrœdinger equation then describes a steady flow of probability current with fixed mass and energy. The generalized forces expressed by the Lagrange multipliers provide momentum at exactly the rate required to offset the scattering by the Board. The more-general fluctuating constraint technique introduced by Nosé could alternatively be used, controlling generalized Lagrange parameters with integral feedback and allowing the mass, momentum, and energy to fluctuate about prescribed mean values. Here we consider explicitly the special case in which these flow quantities are fixed.

It is convenient to solve the Galton Board problem on a hexagonal finite-difference grid. To use such a grid approach, the spatial derivatives are replaced by finite differences. Then the Gaussian equations of motion become a set of coupled nonlinear first-order ordinary differential equations. These equations can be solved using the same Runge-Kutta method that applies for classical problems. Sample solutions, on a 41x41 grid, both transient and time-averaged, are shown in Figures **6-8** on the next page.

Numerical study of the time development of *pairs* of such solutions, initially close together in ψ space, shows that ψ itself does *not* develop in a chaotic way. The separation between such a pair of solutions increases more rapidly than linearly, but less rapidly than exponentially, in time. This intermediate time dependence appears to have no simple power-law behavior. Thus neither the equilbrium nor the nonequilibrium steady-state behavior of ψ provides an analog for classical chaos.

So far we know that solutions of such quantum problems must lead to distributions approaching the fractal classical ones. Further study of the quantum *time*-development will eventually reveal the quantum analog of Lyapunov instability which underlies the Second Law of Thermodynamics and the irreversibility that Boltzmann found to be so fascinating.

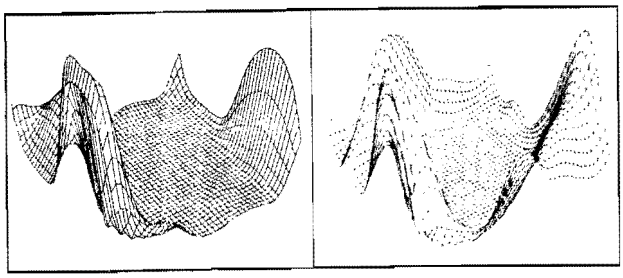

Mass

Figure 6. Mass distribution in a steady-state solution of the quantum Galton Board using the nonequilibrium form of Schrœdinger's Equation described on the previous page. The 41x41 grid is centered on a scatterer which excludes 613 of the 1681 sites from occupancy. The time-dependent Gaussian modification of Schrœdinger's equation is then solved for the 1068 nonvanishing values of the real and imaginary wave-function. In the flow illustrated here, the average flow velocity is about half the thermal velocity, which is in turn about ten times less than the maximum thermal velocity allowed by the finite-difference grid. The quantum-momentum wavelength corresponding to this solution is about 40% of the cell width. The left view is a snapshot of the mass distribution. The right view is a time average over two wave-traversal times.

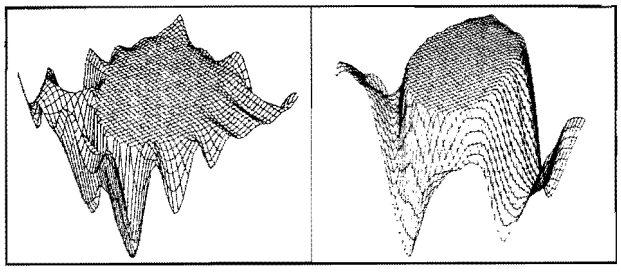

Momentum

Figure 7. Momentum distribution in the steady-state solution of the quantum Galton Board, as shown in Figure 6, using the nonequilibrium Schrœdinger equation described on the previous page. The left view is a snapshot of the momentum distribution. The right view is a time average. The current flow is primarily negative so that the plotted values lie below the zero associated with the 613-site elastic scatterer.

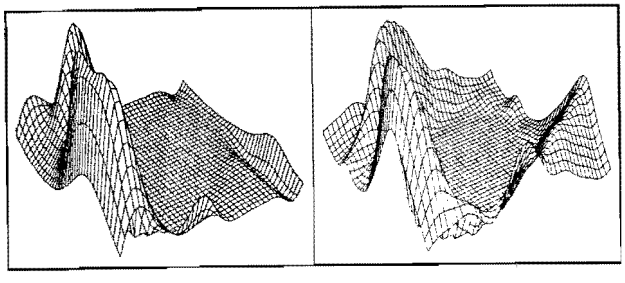

Energy

Figure 8. Energy distribution in a steady-state solution of the quantum Galton Board, as shown in Figure 6, using the nonequilibrium Schrœdinger equation described on the previous page. The left view is a snapshot of the energy distribution. The right view is a time average. Note the similarity of this time average to the mass average shown in Figure 6.

III. Summary.

The averaging introduced by Maxwell and Boltzmann disappeared for a while, with fast computers, but eventually reappeared with a vengeance when both trajectories, described by ordinary differential equations, and distributions, described by partial differential equations, could be found for the same problems. The intercomparison of these two approaches, using ideas based in computation rather than in hand calculation, has led to exciting advances in physics.

The distribution-function analysis of Boltzmann could be tested by the trajectory calculations of Fermi, Alder and Wainwright, Vineyard, Rahman, and Verlet, and, for the first time, validated in cases where the force law was known. The molecular dynamics calculations superceded the interest in approximate one-body and two-body distribution functions and stimulated the advancement of two-body perturbation theory as a way for "understanding" many-body systems. At the same time the realism introduced by Vineyard broadened the audience and has helped make molecular dynamics a useful tool for understanding far-from-equilibrium processes in such diverse fields as catalysis, drug design, fluid dynamics, and materials science.

Nonequilibrium calculations have demonstrated both the power and the limits of linear transport theory and showed that the boundary conditions are crucial in simulating and describing far-from-equilibrium systems. Finally, Nosé's novel approach made it possible to link deterministic microscopic mechanics with phase-space distributions and irreversible thermodynamics, in a way which Boltzmann would have enjoyed.

Where is atomistic computer simulation headed today? A major trend is toward parallel processing, to avoid the speed and capacity limits of a single processor. This approach promises rapid orders-of-magnitude increases in speed and capacity. Another direction in which improving capacity may lead is toward simulating far-from-equilibrium quantum systems. The new techniques may well simplify the treatment of quantum systems which show chaos. It is for this reason that I append Erwin Schrœdinger to the list of precomputer architects of molecular dynamics shown in **Figure 9**, Boltzmann, Gauss, Hamilton, Lyapunov, and Newton.

IIII. Acknowledgment

At Giovanni Ciccotti's suggestion, and with the kind cooperation of Professors Grosse and Posch, of the University of Vienna, this material was first presented in a pair of seminar talks, at the Hohe Wand (Austria) Boltzmann Seminar, in January 1989. My participation in the Seminar was supported by the Austrian Physical Society as well as by the University of California at Davis and at Livermore and the Lawrence Livermore National Laboratory. The work reported here involved the joint efforts and hard work of many people. Of these, Brad Holian, Harald Posch, Bill Moran, Will Evans, Art Walstead, Bill Ashurst, Eckart Meiburg, Peter Cramer, Mark Waid, and my wife, Carol, deserve special thanks.

Figure 9. Boltzmann, Gauss, Hamilton, Lyapunov, Newton, and Schrœdinger.

REFERENCES:

[1]. J. Salmon, Hadronic Journal **3**, 1080(1980).
[2]. S. Nosé, Mol. Phys. **52**, 255(1984) and **57**, 187 (1986).
and J. Chem. Phys. **81**, 511(1984).
[3]. W. G. Hoover, Phys. Rev. **A31**, 1695 (1985).
[4]. W. G. Hoover, Lecture Notes in Physics, Vol. 258, **Molecular Dynamics** (Springer-Verlag, Berlin, 1986).
[5]. D. J. Evans and B. L. Holian, J. Chem. Phys. **83**, 4069(1985).
[6]. B. L. Holian, J. Chem. Phys. **84**, 3138(1986).
[7]. W. G. Hoover, H. A. Posch, B. L. Holian, M. J. Gillan, M. Mareschal, and C. Massobrio, Mol. Sim. **1**, 79(1987).
[8]. B. L. Holian, W. G. Hoover, and H. A. Posch, Phys. Rev. Letts. **59**, 10(1987). B. L. Holian, G. Ciccotti, W. G. Hoover, H. A. Posch, and B. Moran, Phys. Rev. **A** (to appear, 1989).
[9]. W. G. Hoover, Phys. Rev. **A37**, 252(1987).
[10]. J. Gleick, **Chaos, Making a New Science**(Viking, New York, 1987).
[11]. H. G. Schuster, **Deterministic Chaos** (Physik-Verlag, Weinheim, FRG, 1984).
[12]. H. Bai-Lin, **Chaos** (World Scientific, Singapore, 1984).
[13]. J. Ford, "Directions in Classical Chaos", in **Directions in Chaos,** Vol. **1**, p. 1, H. Bai-Lin, ed. (World Scientific, Singapore, 1988).
[14]. B. Mandelbrot, **The Fractal Geometry of Nature** (W. H. Freeman, San Francisco, 1982).
[15]. B. Moran, W. G. Hoover, and S. Bestiale, J. Stat. Phys. **48**, 709 (1987); W. G. Hoover, B. Moran, C. G. Hoover, and W. J. Evans, Physics Letters A, **133**, 114(1988).
[16]. A. J. C. Ladd and W. G. Hoover, J. Stat. Phys. **38**, 973(1985). G. P. Morriss, Phys. Rev. **A** (to appear, 1989).
[17]. G. P. Morriss, J. Stat. Phys. **44**, 107(1986); G. P. Morris, Phys. Lett. **113A**, 269 (1985); G. P. Morriss, Phys. Rev. **A 37**, 2118 (1988).
[18]. W. G. Hoover, H. A. Posch, and S. Bestiale, J. Chem. Phys. **87**, 6665 (1987); H. A. Posch and W. G. Hoover, Phys. Rev. **A38**, 473 (1988); H. A. Posch and W. G. Hoover, Phys. Rev. **A39**, (to appear 1 February, 1989).
[19]. L. A. Pars, **A Treatise on Analytical Dynamics** (Oxbow Press, Woodbridge, Ct., 1979).
[20]. G. Casati, I. Guarneri, and D. L. Shepelyansky, IEEE J. Quant. Electronics **24**, 1420(1988).
[21]. R. W. Hasse, Rep. Prog. Phys. **41**, 1027(1978).
[22]. A. O. Caldeira and A. J. Leggett, Physica **121A**, 587(1983).
[23]. H. Dekker, Phys. Rev. **A 16**, 2126(1977).